Sensors and Actuators B xxx (2017) xxx–xxx

Contents lists available at ScienceDirect

Sensors and Actuators B: Chemical

journal homepage: www.elsevier.com/locate/snb

Research Paper

# Efficient wide range electrochemical bisphenol-A sensor by self-supported dendritic platinum nanoparticles on screen-printed carbon electrode

Kyubin Shim [a], Jeonghun Kim [a], Mohammed Shahabuddin [b], Yusuke Yamauchi [a], Md. Shahriar A. Hossain [a,*], Jung Ho Kim [a,*]

[a] Institute for Superconducting and Electronic Materials (ISEM), Australian Institute for Innovative Materials (AIIM), University of Wollongong, North Wollongong, NSW 2500, Australia
[b] Department of Physics and Astronomy, College of Science, King Saud University, P.O. Box 2455, Riyadh, 11451, Saudi Arabia

ARTICLE INFO

*Article history:*
Received 6 July 2017
Received in revised form 29 August 2017
Accepted 14 September 2017
Available online xxx

*Keywords:*
Nanoporous Pt
Platinum nanoparticles
Electrochemical sensor
Bisphenol A
Electrocatalyst

ABSTRACT

A highly sensitive sensor is strategically designed for bisphenol A (BPA) detection. To enable the sensor to meet the requirements of sensitivity and selectivity, dendritic platinum nanoparticles (DPNs) with a high surface area were prepared and directly coated on gold nanoparticles deposited on a screen-printed carbon electrode, followed by the deposition of a polyethyleneimine-phosphatidylcholine (PEI-PC) layer. The PEI-PC layer protects the sensor against interference effects (such as from ascorbic acid, acetaminophen, uric acid, and dopamine) and further enhances the sensitivity. With our sensor, we were able to detect the presence of bisphenol A precisely at the oxidation potential of 0.270 V. The sensor performance in BPA detection using amperometry under the optimized experimental conditions was demonstrated to reveal the two wide dynamic ranges of 0.01–1.0 μM and 1.0 μM–300 μM, with correlation coefficients of 0.9957 and 0.9864, respectively. The detection limit (DL) for BPA was determined to be 6.63 ± 0.77 nM. To examine its reliability, the sensor was evaluated for the detection of BPA in tap water through a recovery study, which paves the way for practical applications.



## 1. Introduction

Over the past several decades, exposure to chemicals in the environment has been causing various problems for human health. Among the problem chemicals is bisphenol A (BPA, 2,2-bis(4-hydroxyphenyl) propane), which is one of the raw materials used to produce the polycarbonate-based plastics and epoxy resins that are ubiquitous in our daily lives. For example, polycarbonate plastics are used for food containers, drink packaging, and medical devices. In addition, epoxy resins are used to coat metal products (e.g. food cans, bottle tops, etc.). [1,2] Also, The threshold values are set for Bisphenol A in water sample by the European Chemicals Bureau, it has defined the predicted no effect concentration (PNEC) for BPA in freshwater is 1.5 $\mu g\,L^{-1}$ and for marine water is 0.15 $\mu g\,L^{-1}$ [3]. Even though BPA is an estrogenic environmental toxin that can lead to breast cancer, prostate cancer, birth defects, infertility, precocious development in girls, diabetes, and obesity [4,5], the most prevalent polycarbonate-based products still rely on BPA because of its cost-effectiveness. It is thus important to study methods for robust, selective, and sensitive BPA detection.

There have been various analytical methods for the detection of BPA, including separation analysis [6–8], fluorimetry [9,10], immunoassay [11–13], fluorescence [14], field-effect transistor [15], and laser direct writing [16]. These methods, however, demand sophisticated instruments, complex preparation of materials, tedious sample treatment, and long analysis time. Importantly, electrochemical methods can offer inexpensive instruments, short analysis time, simplicity, and great sensitivity. With this background, many electrochemical sensors have been developed to detect BPA using the direct oxidation reaction [17], which requires electrochemically active electrode materials such as carbon [18,19], graphene [14,20], metal oxides [21–23], metal composites [24–26], and metals [27–29]. Since the direct oxidation of BPA may cause the deactivation of carbon or noble metal electrodes by poisoning, it is still a great challenge to develop more reliable, sensitive, and selective approaches. In addition, BPA oxidation occurs at a relatively high potential, lowering the selectivity due to co-oxidation of

* Corresponding authors.
*E-mail addresses:* shahriar@uow.edu.au (Md.S.A. Hossain), jhk@uow.edu.au (J.H. Kim).

http://dx.doi.org/10.1016/j.snb.2017.09.096
0925-4005/

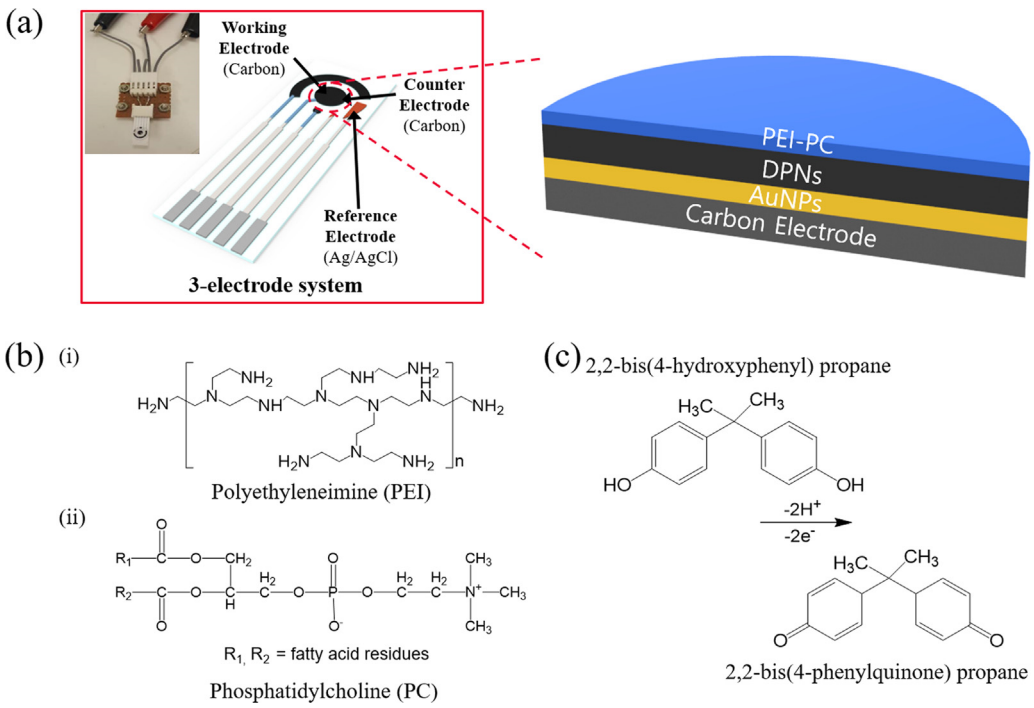


**Fig. 1.** (a) Photograph and schematic illustration of PEI-PC/DPNs/AuNPs electrode. (b) Chemical structures of polyethyleneimine (PEI) and phosphatidylcholine (PC). (c) Bisphenol A oxidation.

interfering species. It is thus necessary to find a new catalytic electrode material to enhance the sensor performance through direct BPA oxidation without electrode poisoning. Such electrode materials, including carbon and various metals or precious metals, have been explored as potential candidates.

Among the candidates, platinum (Pt) as an electrocatalytic material is used in various applications despite its high cost, because it can detect a wide range of various species. [30] After the invention of nanoporous/mesoporous structures with high surface area, noble metals, including Pt, have become highly attractive choices. In particular, they can be applied for the oxidation/detection of some organic species, such as glucose [7,31,32], phenols [28], and methanol [33–35], due to their high catalytic activity and controllable morphology. Recently, Pt nanoparticles with high surface to volume ratios have received much attention because they can provide outstanding electrochemistry performance compared to bulk platinum nanoparticles [36–39]. Based on these advantages, we have introduced dendritic platinum nanoparticles (DPNs) for sensing BPA via its electrochemical oxidation reaction. A BPA sensor using only DPN electrode would be disturbed, however, by some other organic species, which directly affect the oxidization of the DPN layer. Thus, it is necessary to avoid interference from positively charged oxidisable species. One way to avoid the interference and enhance the sensitivity is to coat the DPN surface with a selective polymer layer (polyethyleneimine, PEI) that has a positive charge, and/or lipid molecules (phosphatidylcholine, PC) bearing ammonium and phosphate head groups. BPA in particular bears —OH groups, and they form hydrogen bonds with the head groups of PC, so that the sensor probe coated with a PEI layer having tertiary amine groups can provide additional interaction with BPA.

In the present work, therefore, the DPNs were prepared by the sonochemical method using micelles, and their morphology and structure were carefully characterized. The sensor was prepared with a layer of DPNs-coated Au nanoparticles deposited on a screen-printed carbon electrode, followed by the selective membrane with positive and interactive head groups. Hence, we formed a layer composed of PEI [40] and PC [41] on the DPN surface. The sensor performance of the DPN modified electrode was compared with that of a commercial platinum nanoparticle (Pt black) electrode through electrochemical methods. We also examined the interference effects of foreign species. Finally, the reliability of the as-designed sensor was evaluated using tap water with a view toward practical applications.

## 2. Experimental section

### 2.1. Reagents and materials

Potassium tetrachloroplatinate(II) ($K_2PtCl_4$, 98%), polyethylene glycol hexadecyl ether (Brij 58, $HO(CH_2CH_2O)_{20}C_{16}H_{33}$), L-ascorbic acid (AA, $C_6H_8O_6$, reagent grade) bisphenol A (BPA), polyethyleneimine (PEI), acetaminophen (AP), dopamine (DA), and uric acid (UA) were obtained from Sigma-Aldrich. Platinum black was purchased from Alfa Aesar. Phosphatidylcholine (PC) was purchased from Avanti Polar Lipids, Inc. (USA). Phosphate buffer solution (0.1 M, pH 7.4) was prepared by mixing stock solutions of 0.1 M $NaH_2PO_4$ and 0.1 M $Na_2HPO_4$.

### 2.2. Instruments

A screen-printed carbon electrode (SPCE) was used as a disposable all-solid-state sensor strip for the detection of bisphenol A. The carbon was insulated, with an area of 0.03141 $cm^2$ exposed for the working electrodes. Ag/AgCl was used as the reference electrode and pure carbon was also used as the counter electrode (Fig. 1a) [42,43]. Amperograms and cyclic voltammograms (CVs) were recorded using a potentiostat/galvanostat (Ivium, Netherland and Kosentech, Korea). Detailed microstructures were examined using transmission electron microscopy (TEM) (JEOL-2100, Japan) and scanning electron microscopy (SEM) (Hitachi SU-8000, Japan). Wide-angle powder X-ray diffraction (XRD) patterns were obtained with a GBC MMA XRD at a scanning rate of $2^\circ$ $min^{-1}$. X-ray photoelectron spectroscopy (XPS) was conducted on an ESCALAB 250. The wetting properties of DPNs, PEI/DPNs, and PEI-PC/DPNs sam-

Please cite this article in press as: K. Shim, et al., Efficient wide range electrochemical bisphenol-A sensor by self-supported dendritic platinum nanoparticles on screen-printed carbon electrode, Sens. Actuators B: Chem. (2017), http://dx.doi.org/10.1016/j.snb.2017.09.096

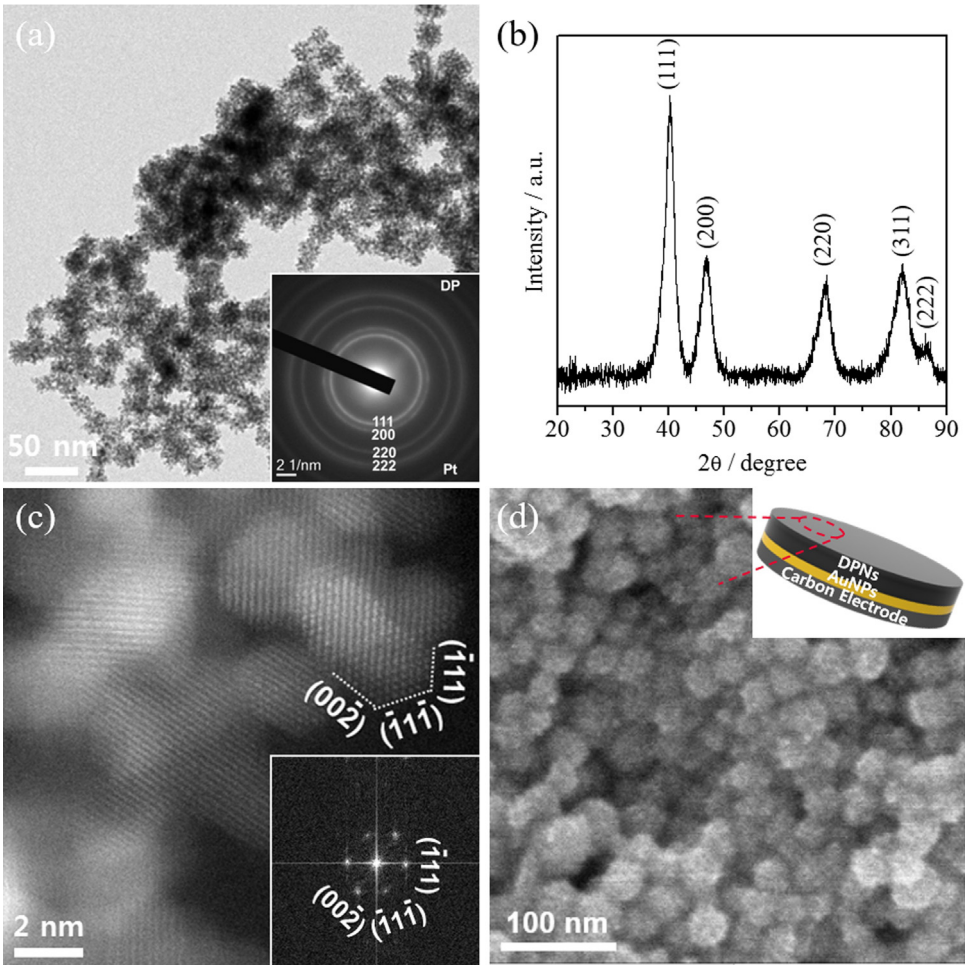


**Fig. 2.** (a) TEM image of prepared DPNs (inset: SAED pattern). (b) Wide-angle XRD pattern of DPN. (c) HAADF-STEM image of DPNs (inset: FFT pattern). (d) SEM image of DPNs/AuNPs on electrode (schematically illustrated in inset).

ples were analysed by a contact angle 101 measurement system (PSM Company). The minimized energy between BPA and PC was calculated using Chem3D pro12.0 (PerkinElmer Informatics) and the obtained chemical structures at minimized energy state were described in Fig. 5(a).

### 2.3. Preparation of dendritic platinum nanoparticles (DPNs)

For the preparation of the DPNs, we used the following solutions: 5 ml of 20 mM $K_2PtCl_4$ aqueous solution, 1 ml of 50 mg Brij® 58 aqueous solution, and 5 ml of 0.1 M ascorbic acid (AA) aqueous solution, respectively, with each solution kept at room temperature (20 °C). The $K_2PtCl_4$ and Brij 58 solutions were mixed in another vessel, and subsequently, the AA aqueous solution was added. The mixed solution was reacted at room temperature (20 °C) for 50 min under ultrasonication (220–240 V, 50–60 Hz). The precipitates were collected by centrifugation and washed several times with deionized (DI) water to remove the surfactant and excess reactants [44].

### 2.4. Preparation of gold nanoparticles (AuNPs)

For the preparation of the colloidal gold solution, 1 ml of $HAuCl_4{\cdot}3H_2O$ (1 wt%) was stirred into 90 ml deionized water for 1 min, and then 2 ml of 38.8 mM sodium citrate was added to the solution with stirring for 1 min. Following this, 1 ml of fresh 0.075 wt% $NaBH_4$ in 38.8 mM sodium citrate solution was added very slowly with continuous stirring. The reaction mixture was allowed to stand for 15–20 min and then used without purification [45].

### 2.5. Preparation of PEI-PC/DPNs/AuNPs electrode

AuNPs (as prepared solution), DPNs (1 mg ml$^{-1}$), and PEI-PC membrane solutions were sequentially coated on a screen-printed carbon electrode, and the as-prepared electrode was dried in an oven at 55 °C: Firstly, the gold nanoparticles (AuNPs) were dropped onto the screen-printed carbon electrode (SPCE) and were dried. Secondly, the dendritic platinum nanoparticles (DPNs) were dropped on the AuNP modified SPCE and were dried. The electrode surface was then activated by potential cycling from −0.55 V to 1.1 V with a scan rate of 0.2 V s$^{-1}$ for 30 cycles in 0.5 M sulfuric acid, and washed with distilled water (DI water). Finally, a membrane solution prepared by mixing PEI (0.5%) with PC (0.5 mM) (95 wt%: 5 wt%) was coated on the DPNs/AuNPs/SPCE and used for the experiments.

## 3. Results and discussion

To demonstrate the performance of the sensor using dendritic platinum nanoparticles (DPNs) for bisphenol A (BPA) detection, we strategically designed a three-layer electrode architecture, with the layers (from the top down) consisting of polyethyleneimine/phosphatidylcholine (PEI-PC), DPNs,

Please cite this article in press as: K. Shim, et al., Efficient wide range electrochemical bisphenol-A sensor by self-supported dendritic platinum nanoparticles on screen-printed carbon electrode, Sens. Actuators B: Chem. (2017), http://dx.doi.org/10.1016/j.snb.2017.09.096

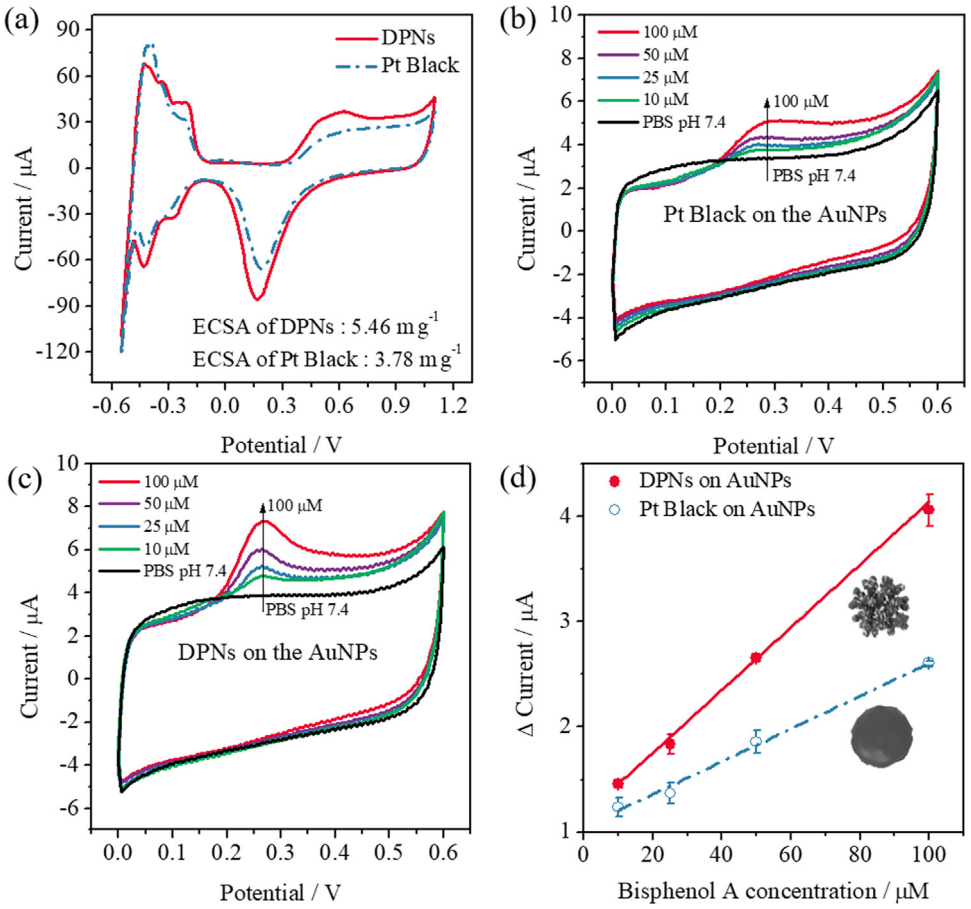


**Fig. 3.** Cyclic voltammograms (CVs) for characterization of DPNs and Pt Black on the AuNPs modified electrodes. (a) Determination of electrochemical active surface area (ECSA) of DPNs and Pt Black. (b) Detection of various concentrations (10, 25, 50, and 100 μM) of bisphenol A using Pt Black electrode. (c) Detection of various concentrations (10, 25, 50, and 100 μM) of bisphenol A using DPNs electrode. (d) Bisphenol A detection calibration curves (DPNs and Pt black), with insets showing DPN and Pt Black particles. (For interpretation of the references to colour in the text, the reader is referred to the web version of this article.)

and gold nanoparticles (AuNPs), respectively (denoted as PEI-PC/DPNs/AuNPs). Herein, the purpose of the PEI-PC was to enhance sensitivity and to reduce the interference effect on the BPA sensor. The AuNPs were also used for stabilization of the screen-printed carbon electrode (SPCE). A photograph of the set-up and a detailed illustration of the PEI-PC/DPNs/AuNPs on the SPCE are clearly shown in Fig. 1a. Fig. 1b displays the chemical structures of the components of PEI-PC, which can offer enhancement of the sensor's selectivity and sensitivity due to their polarity and charge properties [46,47]. In the as-prepared electrode, the bisphenol A is detected from its electrochemical oxidation reaction, a two-electron and two-proton process, in which it is converted to 2,2-bis(4-phenylquinone) propane (Fig. 1c).

The structure of the DPNs prepared by the sonochemical method was observed by transmission electron microscopy (TEM) as shown in Fig. 2. The as-prepared DPNs showed a dendritic structure with an abundance of pores 2–4 nm in size, which offer highly catalytic sites. The average size of the DPNs was estimated to be around 25 nm (Fig. 2a). The selected area diffraction pattern (SAED) in the inset confirmed that the particles have a typical face-centred-cubic (*fcc*) structure. In detail, the particles show concentric rings representing the (111), (200), (220), and (222) planes. This is further supported by the wide-angle X-ray diffraction (XRD) pattern, which exactly corresponds to the *fcc* structure (Fig. 2b). From detailed high-angle annular dark field scanning TEM (HAADF-STEM) analysis, the {111} and {200} facets were observed in various beam orientations using fast Fourier transform (FFT) patterns (inset in Fig. 2c). Based on this information, the DPNs were directly deposited on the AuNPs/carbon electrode. As can be seen in Fig. 2d, the top-view scanning electron microscope (SEM) image provides the evidence of the successful coverage by DPNs. The DPN-coated electrode is composed of particles with homogeneous shapes and sizes.

The electrochemical active surface areas (ECSA) of the DPNs and commercial Pt black powders were closely compared using cyclic voltammetry (CV) in the range of −0.55 V to +1.1 V (vs. Ag/AgCl) in a 0.5 M sulfuric acid ($H_2SO_4$) solution at the scan rate of 0.1 V $s^{-1}$. We observed that the DPNs possessed a relatively high hydrogen adsorption/desorption currents compared to the Pt black. From the results, the ECSA determined for DPNs was 5.46 $m^2$ $g^{-1}$, while that for the Pt black was estimated to be 3.78 $m^2$ $g^{-1}$ (Fig. 3a), indicating that the DPNs had more catalytic active sites. We propose that the DPNs reveal an enhanced current response for BPA due to their highly catalytic surfaces and sites.

The as-prepared electrode was further tested for electrochemical BPA detection. Before the determination of BPA, two DPNs (or Pt black)/AuNPs/carbon electrodes were first activated by scanning the potential from 0.0 V to 0.6 V at a scan rate of 0.1 V $s^{-1}$ for 20 cycles. Through this step, it allows the stabilization of the baseline and the electrodes can get more reproducible response. After the electrodes were activated, CVs were recorded in various concentrations of BPA by scanning the potential from 0.0 V to 0.6 V at a scan rate of 0.1 V $s^{-1}$. During the scan to the positive direction to +0.6 V from 0.0 V, the voltammetric responses of the Pt black (Fig. 3b) and DPNs (Fig. 3c) powders to BPA in a phosphate buffered saline (PBS) buffer solution revealed a clear oxidation peak at around +0.27 V vs.

Please cite this article in press as: K. Shim, et al., Efficient wide range electrochemical bisphenol-A sensor by self-supported dendritic platinum nanoparticles on screen-printed carbon electrode, Sens. Actuators B: Chem. (2017), http://dx.doi.org/10.1016/j.snb.2017.09.096

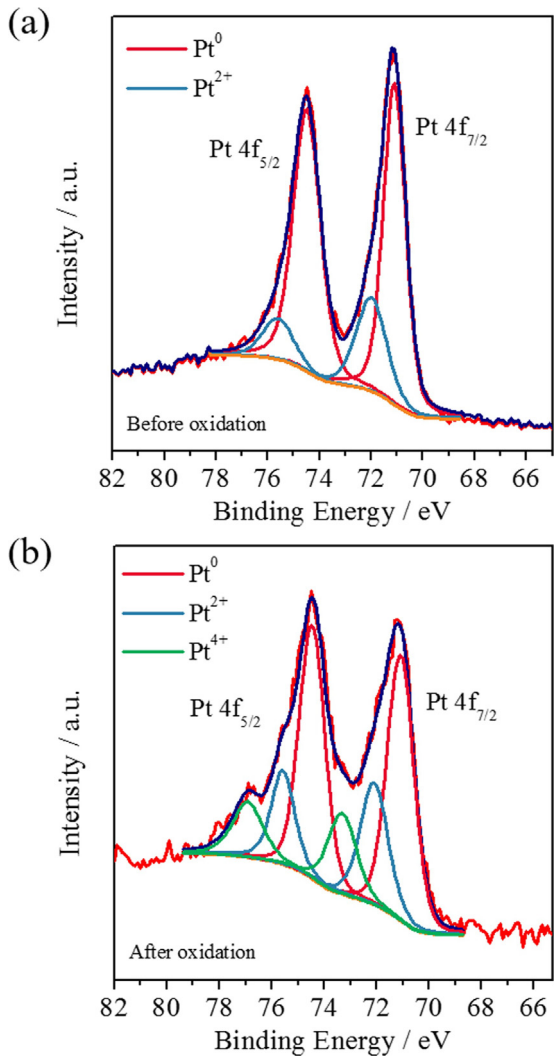


**Fig. 4.** XPS analysis of surface of DPNs electrode: (a) before BPA oxidation, (b) after BPA oxidation.

Ag/AgCl (sat. KCl) (Fig. 3b and c) in both cases, while no redox peaks were observed on either electrode in a blank PBS solution. From the results, the obtained response current of the DPNs was about two times higher than that of the Pt black. In addition, the calibration plots showed that the sensitivity of the DPNs modified electrode (slope = 0.0298 $\mu A\ \mu M^{-1}$) (red) is 2 times higher than that of the Pt black modified electrode (slope = 0.0155 $\mu A\ \mu M^{-1}$) (blue) (Fig. 3d). These results indicate that the DPNs electrode has much better BPA sensing capability than commercially available Pt black electrodes. As a result, our DPNs were clearly worth applying on a BPA sensor.

To further characterize its working principle as a BPA sensor, we also evaluated the surface conditions of the DPNs modified electrode. For this purpose, detailed XPS spectra were obtained for the DPNs electrode before and after the oxidation of BPA in the phosphate buffer solution (PBS), as can be seen in Fig. 4a and b. The XPS spectra of the DPNs modified electrode revealed peaks at 74.49 eV, 71.10 eV ($Pt^0$); and 75.6, 71.99 eV ($Pt^{2+}$) before the oxidation (Fig. 4a). After the BPA oxidation, peaks were observed at 74.45 eV, 71.07 eV ($Pt^0$); 75.57 eV, 72.09 eV ($Pt^{2+}$); and 76.91 eV, 73.31 eV ($Pt^{4+}$) (Fig. 4b). It should be noted that an additional peak ($Pt^{4+}$) was clearly present after the BPA oxidization on the DPNs electrode. That is to say, both $Pt^0$ and air-oxidized $Pt^{2+}$ at the DPNs surface are partially oxidized to $Pt^{4+}$ during the oxidation of BPA. This result can support an electrochemical oxidation reaction of the BPA, as described in Fig. 1c. The detailed electrochemical surface properties of different electrodes in negatively charged $K_3Fe(CN)_6$ and positively charged $[Ru(NH_3)_6]Cl_3$ solutions are provided in the Supplementary materials (Fig. S1).

Finally, we also needed to confirm the surface oxidization and surface morphology of DPNs with and without PEI-PC. From the SEM observations, the surface was composed of homogeneously dispersed DPNs before deposit of the PEI-PC layer (Fig. S2a), while a murky image of DPNs was observed after the PEI-PC layer coating (Fig. S2c). That is to say, there is an obvious thin coating layer of PEI-PC on the DPNs. The formation of each layer was additionally confirmed using XPS (Fig. S2b and d). The XPS spectra obtained for the PEI-PC layer showed O1s, N1s, and C1s peaks with relatively strong intensity after PEI-PC coating, while the XPS intensity of Pt 4f was relatively decreased. This indicates that the PEI-PC layer covered the electrode surface completely.

As was described above, to improve the sensitivity and reduce interference effects, the DPNs/AuNPs/SPCE (denoted as DPNs-modified electrode) was covered with a functional layer, which was drop-coated by mixed solutions of PEI and PC with different weight percentages. Anion permeation can be achieved by covering the electrode with a positively charged PEI layer to protect it from interference by other species [40]. Otherwise, the PC, having both positively charged-tertiary amine and negatively charged-phosphate groups in the head part, would give the coating a neutral property [41]. In addition, the tail group of the PC molecule has a hydrophobic property that can protect the sensor from other hydrophilic interfering species, and also, the head group of PC can form a hydrogen bond with the —OH group of BPA to enhance the sensitivity of the sensor. Theoretically, a highly sensitive layer can be designed through the orientation of the head group of the PC so that it faces inward and the tail part faces outward on the PEI layer. Based on these considerations, the selectivity and sensitivity to the target species was improved, so that the interference effect by positively charged molecules was reduced, and the hydrogen bond formation between the head groups of PC and BPA could enhance the sensitivity. To support our hypothesis about the complex interaction between the BPA and the PC, their interactions were studied by calculating the minimized energy. The interaction of deprotonated phenyl groups of BPA and $(CH_3)_3N^+$ groups of PC was expected to be stable (Fig. 5a). Therefore, the rationally design sensor can be fabricated using a PEI-PC layer. To evaluate its reliability, CVs were recorded for a sample solution containing bioorganic interfering molecules, such as dopamine, and the sensor showed a reduced response for positively charged interfering species. This indicates that the PEI-PC layer plays an important role in protecting the sensor from interference effects and improving sensitivity.

Most conventional electrodes composed of various metal nanoparticles have the drawbacks that they simultaneously detect mixed species, including ascorbic acid (AA), acetaminophen (AP), uric acid (UA), and dopamine (DA), even at different oxidation potentials. With this background, our strategic PEI-PC coating was introduced onto the DPNs-modified electrode due to its selectively oxidized functionality and minimization of interference effects. To obtain the best response from the PEI-PC/DPNs/AuNPs, therefore, the experimental conditions were systematically optimized in terms of the amount of DPNs, the concentration of PEI, and the ratio of PC to PEI (Fig. S3). In regard to the amount of DPNs, 3 μl (1 mg $ml^{-1}$) of DPNs was drop-coated on the AuNPs deposited on the SPCE from one to four times, as can be seen in Supporting Information Fig. S3a. In detail, the CVs (not shown here) were evaluated for the DPNs-modified electrodes with different amounts of DPNs (3 μl–12 μl) in PBS solution containing various concentrations of BPA (2.5 μM–10 μM). The results clearly revealed that the elec-

Please cite this article in press as: K. Shim, et al., Efficient wide range electrochemical bisphenol-A sensor by self-supported dendritic platinum nanoparticles on screen-printed carbon electrode, Sens. Actuators B: Chem. (2017), http://dx.doi.org/10.1016/j.snb.2017.09.096

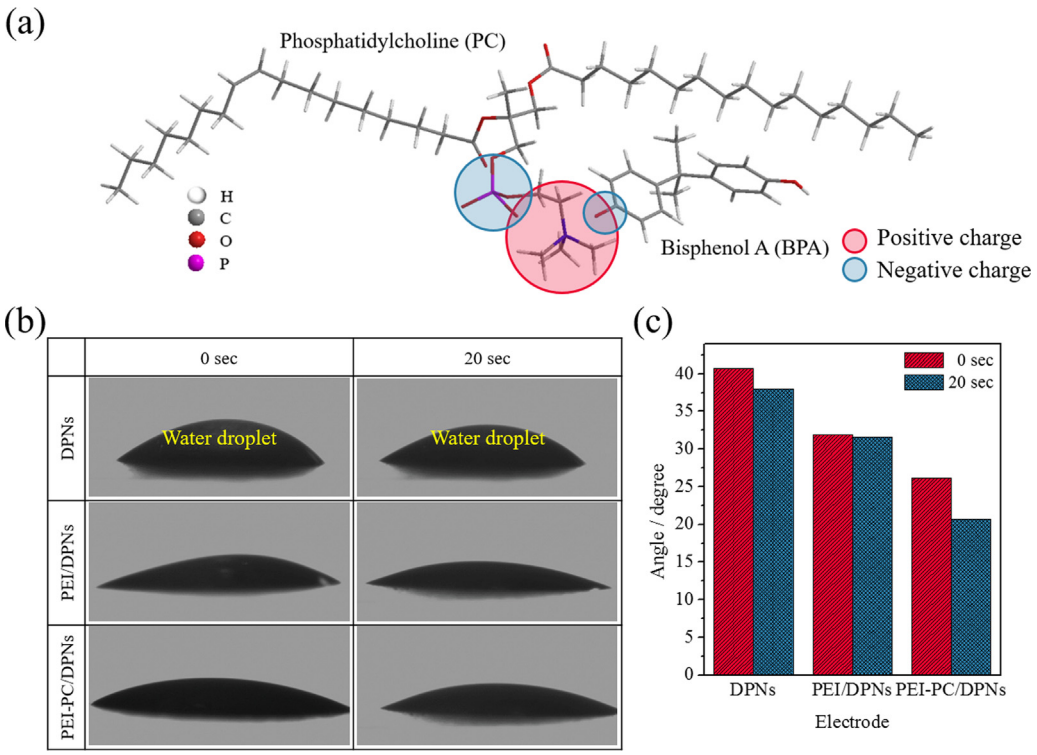


**Fig. 5.** (a) The chemical structure of interaction of between BPA and PC at minimized energy. (b) Photographs of water contact angles of various layers (DPNs, PEI/DPNs, and PEI-PC/DPNs). (c) Contact angles of various layers (DPNs, PEI/DPNs, and PEI-PC/DPNs).

trode coated with 3 μl (1 mg ml$^{-1}$) of DPNs gave us the steepest calibration slope.

The effect of PEI concentration on the response current was investigated between 0.1 and 1.5% in 100 μM of BPA solution (Fig. S3b). In this case, 0.5% PEI minimized the decrease in the current response. As was mentioned above, however, using only PEI was not enough to avoid interference and to give more selectivity. Hence, the DPNs surface was covered with a lipid (PC) layer along with the PEI, where the —OH group of BPA was more interactive to the head group of PC molecules through the hydrogen bond formation. To optimize theis, the weight (wt.%) ratio of PEI to PC was varied on the DPNs layer. As shown in Fig. S3c, the maximum response and selectivity toward BPA were observed for the sensor probe with a ratio of 95: 5 wt.% (PEI:PC), which was finally applied to the subsequent experiments.

To confirm the adaptability of as-optimized polymer layers (PEI-PC), we evaluated the sample solution permeability for different layer architectures. The water contact angle for all samples was measured at time intervals of 0 and 20 s, (Fig. 5b). The angles for three samples at 0 s and 20 s were 40.7°and 38° (DPNs); 31.9° and 31.6° (PEI/DPNs); 26.2° and 20.7° (PEI-PC/DPNs), respectively (Fig. 5c). This suggests that the wettable nature of the DPNs surface also increases with the surface modification using PEI and PC. In particular, the PEI-PC/DPNs layer reveals the lowest contact angle, which is the best condition. In addition, the wetting property for all samples was further increased with increasing wetting time, which indicates the better interaction of target species in the solution to be measured with increasing time. With this experimental result, the PEI-PC layer can give us greater responsiveness.

Finally, the interference effects on BPA detection using the PEI-PC/DPNs/AuNPs/SPCE sensor probe were further investigated with 0.5% PEI and 0.5% PEI with PC (0.5 mM phosphatidylcholine, ratio 0.5% PEI (95 wt%) and PC (5 wt%)). In addition, only the DPNs electrode was tested as reference. After electrode activation, the amperometric responses for the oxidation of BPA and the expected

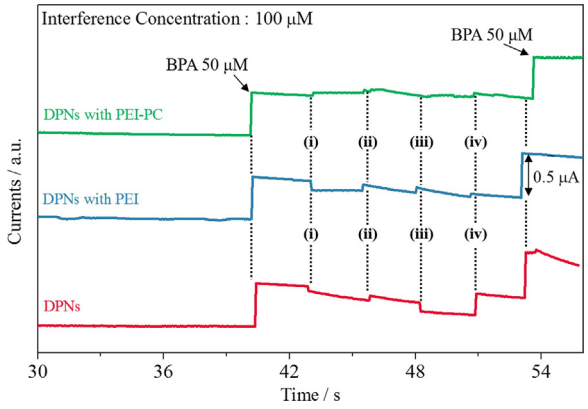


**Fig. 6.** Amperograms of the addition of 50 μM BPA and 100 μM of other interfering species in various electrodes (i: ascorbic acid, ii: acetaminophen, iii: uric acid, and iv: dopamine).

interfering species were assessed between the initial potential of 0.0 V and the final potential of 0.4 V: bisphenol A (BPA) as a reference, and (i) ascorbic acid (AA), (ii) acetaminophen (AP), (iii) uric acid (UA), and (iv) dopamine (DA) (Fig. 6). All the interference was decreased in the order of DPNs/AuNPs, PEI/DPNs/AuNPs, and PEI-PC/DPNs/AuNPs layers. The interference effects were investigated for AA, AP, UA, and DA a reduction in response current was observed on AA (14%), AP (24%), UA (35%), and DA (22%), respectively. After only PEI coating, the response current was somewhat decreased compared to that of bare DPNs, where the percent ratios of the response current were AA (13%), AP (16%), UA (22%), and DA (18%), respectively. On the other hand, the PEI-PC coated-electrode showed a greatly decreased interference effect for AA (4%), AP (3%), UA (5%), and DA (3%) (Fig. 6). The electrodes with only a PEI layer showed high-interference responses (over 10%), while the PEI-PC

Please cite this article in press as: K. Shim, et al., Efficient wide range electrochemical bisphenol-A sensor by self-supported dendritic platinum nanoparticles on screen-printed carbon electrode, Sens. Actuators B: Chem. (2017), http://dx.doi.org/10.1016/j.snb.2017.09.096

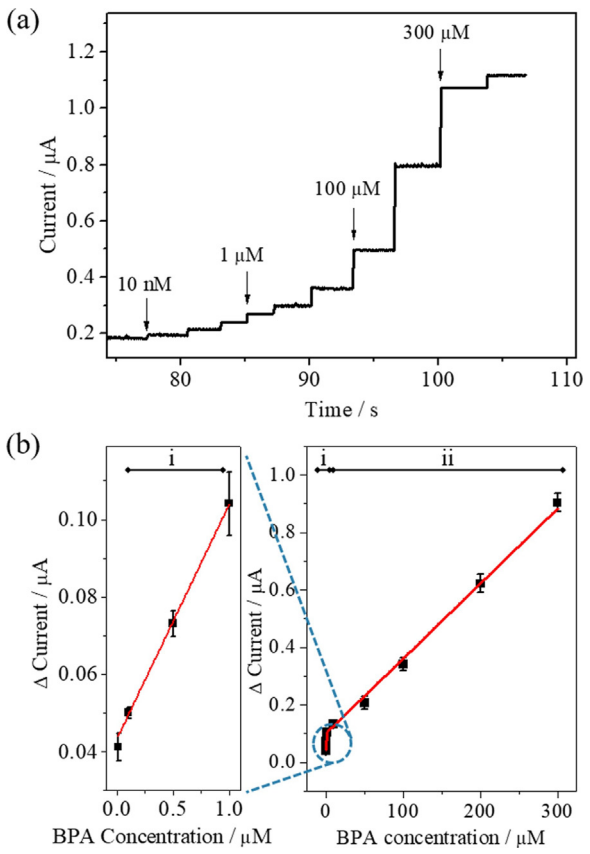


**Fig. 7.** (a) Amperometric response of PEI-PC/DPNs/AuNPs modified SPCE according to different concentrations of BPA. (b) Calibration curves from the amperometric responses at two ranges of BPA concentration: of (i) 0.01–1 μM and (ii) 1–300 μM.

modified electrode displayed low-interference responses (below 5%).

A typical current response curve was observed during successive addition of various concentrations of BPA in a 0.1 M PBS solution using chronoamperometry (CA) (Fig. 7a). In detail, the stepping potential of 0.4 V was applied to obtain amperograms of the BPA sensor probe with the PEI-PC/DPNs/AuNPs architecture. Two dynamic ranges of the calibration plot for the BPA detection were determined from 0.01 to 1.0 μM and from 1.0 μM to 300 μM with respective correlation coefficients of 0.9957 and 0.9864, respectively (Fig. 7b). Two different linear ranges are due to the different kinetics at different concentrations of BPA. The oxidation kinetics in the low concentration range was related to only adsorption process, and the oxidation process at high concentration range depended on adsorption and diffusion of BPA [48,49]. The detection limit (DL) of BPA was determined to be 6.63 ± 0.77 nM. Compared to previous reports [19,23,24,26,29,50–57], the DL reported in this work was quite comparable to those for other sensing materials using the direct oxidation method (Table 1). In order to investigate its reliability, we also investigated the PEI-PC/DPNs/AuNPs modified electrode for the detection of BPA in tap water through a recovery study. Blank solutions were mixed from tap water and PBS in the ratio of 1:1, and three different concentrations of BPA were obtained by mixing it with the blank solution. In this case, the range of recovery was from 95% to 104% (Table 2), indicating that our sensor design paves the way toward practical application.

## 4. Conclusions

We have successfully fabricated and evaluated the highly catalytic dendritic platinum nanoparticles (DPNs) for detection of bisphenol A (BPA). As-prepared DPNs having a high surface area showed very selective and sensitive detection as the sensor. Moreover, the interference effect was obviously reduced by top coating of PEI and PC. Finally, our sensor was further tested in a tap water through recovery study toward practical applications.

**Table 1**
Comparison of proposed sensors for detection of BPA by the electrochemical method (direct oxidation).

| Active materials | Linear range | Detection limit | References |
|---|---|---|---|
| DPNs | 0.01–1, 1–300 μM | 6.6 nM | This work |
| MCM-41 | 0.088–0.22 μM | 38 nM | 23 |
| Pt/Gr-CNTs | 0.06–10.0 μM | 42 nM | 24 |
| AuNPs/$MoS_2$ | 0.05–100 μM | 5 nM | 26 |
| Pd@$TiO_2$-SiC | 0.01–5, 5–200 μM | 4.3 nM | 29 |
| MWCNTs-PEI | 0.01–50 μM | 3.3 nM | 19 |
| Arg-G | 0.005–40 μM | 1.1 nM | 50 |
| Laccase-Thionine-Carbon black | 0.5–50 μM | 200 nM | 51 |
| MWCNTs | 4.9–82.5 μM | 84 nM | 52 |
| $ZrO_2$/Nano-ZSM-5 | 0.006–600 μM | 3 nM | 53 |
| Na-doped $WO_3$ | 0.081–22.5 μM | 28 nM | 54 |
| AuPdNPs/GNs | 0.05–10 μM | 8 nM | 55 |
| AuNP/PVP/PGE | 0.03–1.1 μM | 1 nM | 56 |
| GO/MWCNT | 0.05–1, 1–650 μM | 4.4 nM | 57 |

Gr-CNT (Graphene-carbon), MCM-41 (Mesoporous silica), AuNPs (Gold nanoparticles), MWCNTs (Multi-walled carbon nanotubes), PEI (Polyethylenimine), Arg-G (Arginine functionalized graphene), Nano-ZSM-5 (Nanocrystalline ZSM-5 zeolite), GNs (Graphene nanosheets), PVP (polyvinylpyrrolidone), PGE (pencil graphite electrode), GO (graphene oxide), MWCNT (multiwalled carbon nanotubes).

**Table 2**
Recovery of spiked BPA in tap water. RSD: relative standard deviation.

| Sample | Spiked (μM) | Found (μM) | Recovery (%) | RSD (%) |
|---|---|---|---|---|
| Tap water | 1 | 0.95 | 94.55 | 3.06 |
| | 5 | 5.13 | 102.63 | 2.65 |
| | 10 | 10.39 | 103.90 | 6.77 |

## Acknowledgment

The authors extend their appreciation to The International Scientific Partnership Programme at King Saud University for funding this research work through ISPP #0095.

## Appendix A. Supplementary data

Supplementary data associated with this article can be found, in the online version, at http://dx.doi.org/10.1016/j.snb.2017.09.096.

## References

[1] H. Yin, L. Cui, S. Ai, H. Fan, L. Zhu, Electrochemical determination of bisphenol A at Mg-Al-$CO_3$ layered double hydroxide modified glassy carbon electrode, Electrochim. Acta 55 (2010) 603–610.
[2] H. Yoshida, H. Harada, H. Nohta, M. Yamaguchi, Liquid chromatographic determination of bisphenols based on intramolecular excimer-forming fluorescence derivatization, Anal. Chim. Acta 488 (2003) 211–221.
[3] G.M. Klečka, C.A. Staples, K.E. Clark, N.V.D. Hoeven, D.E. Thomas, S.G. Hentges, Exposure analysis of bisphenol A in surface water systems in north America and Europe, Environ. Sci. Technol. 43 (2009) 6145–6150.
[4] L.N. Vanderberg, R. Hauser, N. Marcus, W.V. Welshons, Human exposure to bisphenol a (BPA), Reprod. Toxicol. 24 (2007) 139–177.
[5] H. Mielke, U. Gundert-Remy, Bisphenol A levels in blood depend on age and exposure, Toxicol. Lett. 190 (2009) 32–40.
[6] Z. Kuklenyik, J. Ekong, C.D. Cutchins, L.L. Needham, A.M. Calafat, Simultaneous measurement of urinary bisphenol A and alkylphenols by automated solid-phase extractive derivatization gas chromatography/mass spectrometry, Anal. Chem. 75 (2003) 6820–6825.
[7] E. Maiolini, E. Ferri, A.L. Pitasi, A. Montoya, M.D. Giovanni, E. Errani, S. Girotti, S. Bisphenol, A determination in baby bottles by chemiluminescence enzyme-linked immunosorbent assay, lateral flow immunoassay and liquid chromatography tandem mass spectrometry, Analyst 139 (2014) 318–324.

Please cite this article in press as: K. Shim, et al., Efficient wide range electrochemical bisphenol-A sensor by self-supported dendritic platinum nanoparticles on screen-printed carbon electrode, Sens. Actuators B: Chem. (2017), http://dx.doi.org/10.1016/j.snb.2017.09.096

[8] H.-B. Noh, P. Chandra, Y.-J. Kim, Y.-B. Shim, A simple separation method with a microfluidic channel based on alternating current potential modulation, Anal. Chem. 84 (2012) 9738–9744.
[9] X. Wang, H. Zeng, L. Zhao, J.-M. Lin, Selective determination of bisphenol A (BPA) in water by a reversible fluorescence sensor using pyrene/dimethyl β-cyclodextrin complex, Anal. Chim. Acta 556 (2006) 313–318.
[10] J. Fan, H. Guo, G. Liu, P. Peng, Simple and sensitive fluorimetric method for determination of environmental hormone bisphenol A based on its inhibitory effect on the redox reaction between peroxyl radical and rhodamine 6G, Anal. Chim. Acta 585 (2007) 134–138.
[11] J. Zhang, S.-Q. Zhao, K. Zhang, J.-Q. Zhou, Cd-doped ZnO quantum dots-based immunoassay for the quantitative determination of bisphenol A, Chemosphere 95 (2014) 105–110.
[12] M.-H. Piao, H.-B. Noh, M.A. Rahman, M.-S. Won, Y.-B. Shim, Label-free detection of bisphenol A using a potentiometric immunosensor, Electroanalytical 20 (2008) 30–37.
[13] M.A. Rahman, M.J.A. Shiddiky, J.-S. Park, Y.-B. Shim, An impedimetric immunosensor for the label-free detection of bisphenol A, Biosens. Bioelectron. 22 (2007) 2464–2470.
[14] Y. Zhu, Y. Cai, L. Xu, L. Zheng, L. Wang, B. Qi, C. Xu, Building an aptamer/graphene oxide FRET biosensor for one-step detection of bisphenol A, ACS Appl. Mater. Interfaces 7 (2015) 7492–7496.
[15] S.G. Kim, S.L. Lee, J. Jun, D.H. Shin, J. Jang, Ultrasensitive bisphenol a field-effect transistor sensor using an aptamer-modified multichannel carbon nanofiber transducer, ACS Appl. Mater. Interfaces 8 (2016) 6602–6610.
[16] C. Cheng, S. Wang, J. Wu, Y. Yu, R. Li, S. Eda, J. Chen, G. Feng, B. Lawrie, A. Hu, Bisphenol A sensors on polyimide fabricated by laser direct writing for onsite river water monitoring at attomolar concentration, ACS Appl. Mater. Interfaces 8 (2016) 17784–17792.
[17] K.V. Ragavan, N.K. Rastogi, M.S. Thakur, Sensors and biosensors for analysis of bisphenol-A, TrAC Trends Anal. Chem. 52 (2013) 248–260.
[18] J.A. Rather, K.D. Wael, Fullerene-$C_{60}$ sensor for ultra-high sensitive detection of bisphenol-A and its treatment by green technology, Sens. Actuators B: Chem. 176 (2013) 110–117.
[19] Y. Yang, H. Zhang, C. Huang, N. Jia, MWCNTs-PEI composites-based electrochemical sensor for sensitive detection of bisphenol A, Sens. Actuators B: Chem. 235 (2016) 408–413.
[20] H. Fan, Y. Li, D. Wu, H. Ma, K. Mao, D. Fan, B. Du, Q. Wei, Electrochemical bisphenol A sensor based on N-doped graphene sheets, Anal. Chim. Acta 711 (2012) 24–28.
[21] L. Hu, C.-C. Fong, X. Zhang, L.L. Chan, P.K.S. Lam, P.K. Chu, K.-Y. Wong, M. Yang, Au nanoparticles decorated $Tio_2$ nanotube arrays as a recyclable sensor for photoenhanced electrochemical detection of bisphenol A, Environ. Sci. Technol. 50 (2016) 4430–4438.
[22] C. Hou, W. Tang, C. Zhang, Y. Wang, N.A. Zhu, A. novel and sensitive electrochemical sensor for bisphenol A determination based on carbon black supporting ferroferric oxide nanoparticles, Electrochim. Acta 144 (2014) 324–331.
[23] F. Wang, J. Yang, K. Wu, Mesoporous silica-based electrochemical sensor for sensitive determination of environmental hormone bisphenol A, Anal. Chim. Acta 638 (2009) 23–28.
[24] Z. Zheng, Y. Du, Z. Wang, Q. Feng, C. Wang, Pt/graphene-CNTs nanocomposite based electrochemical sensors for the determination of endocrine disruptor bisphenol A in thermal printing papers, Analyst 138 (2013) 693–701.
[25] D. Pan, Y. Gu, H. Lan, Y. Sun, H. Gao, Functional graphene-gold nano-composite fabricated electrochemical biosensor for direct and rapid detection of bisphenol A, Anal. Chim. Acta 853 (2015) 297–302.
[26] K.-J. Huang, Y.-J. Liu, Y.-M. Liu, L.-L. Wang, Molybdenum disulfide nanoflower-chitosan-Au nanoparticles composites based electrochemical sensing platform for bisphenol A determination, J. Hazard. Mater. 276 (2014) 207–215.
[27] R. Wannapob, P. Thavarungkul, S. Dawan, A. Numnuam, W. Limbut, P. Kanatharana, A simple and highly stable porous gold-based electrochemical sensor for bisphenol A detection, Electroanalysis 28 (2016) 1–10.
[28] Z. Zheng, J. Liu, M. Wang, J. Cao, L. Li, C. Wang, N. Feng, Selective sensing of bisphenol A and bisphenol S on platinum/poly(diallyl dimethyl ammonium chloride)-diamond powder hybrid modified glassy carbon electrode, J. Electrochem. Soc. 163 (2016) B192–B199.
[29] L. Yang, H. Zhao, S. Fan, B. Li, C.-P. Li, A highly sensitive electrochemical sensor for simultaneous determination of hydroquinone and bisphenol A based on the ultrafine Pd nanoparticle@$TiO_2$ functionalized SiC, Anal. Chim. Acta 852 (2014) 28–36.
[30] M. Malgras, H. Ataee-Esfahani, H. Wang, B. Jiang, C. Li, K.C.-W. Wu, J.H. Kim, Y. Yamauchi, Nanoarchitectures for mesoporous metals, Adv. Mater. 28 (2016) 993–1010.
[31] Q. Shen, L. Jiang, H. Zhang, Q. Min, W. Hou, J.-J. Zhu, Three-dimensional dendritic Pt nanostructures: sonoelectrochemical synthesis and electrochemical applications, J. Phys. Chem. C 112 (2008) 16385–16392.
[32] X. Niu, H. Zhao, C. Chen, M. Lan, Enhancing the electrocatalytic activity of Pt-Pd catalysts by introducing porous architectures, ChemCatChem 5 (2013) 1416–1425.
[33] D.-S. Park, M.-S. Won, R.N. Goyal, Y.-B. Shim, The electrochemical sensor for methanol detection using silicon epoxy coated platinum nanoparticles, Sens. Actuators B: Chem. 174 (2012) 45–50.
[34] M. Rauber, I. Alber, S. Müller, R. Neumann, O. Picht, C. Roth, A. Schökel, M.E. Toimil-Molares, W. Ensinger, Highly-ordered supportless three-dimensional nanowire networks with tunable complexity and interwire connectivity for device integration, Nano Lett. 11 (2011) 2304–2310.
[35] S.M. Alia, G. Zhang, D. Kisailus, D. Li, S. Gu, K. Jensen, Y. Yan, Porous platinum nanotubes for oxygen reduction and methanol oxidation reactions, Adv. Funct. Mater. 20 (2010) 3742–3746.
[36] L. Wang, Y. Yamauchi, Block copolymer mediated synthesis of dendritic platinum nanoparticles, J. Am. Chem. Soc. 131 (2009) 9152–9153.
[37] L. Wang, Y. Yamauchi, Autoprogrammed synthesis of triple-layered Au@Pd@Pt core-shell nanoparticles consisting of a Au@Pd bimetallic core and nanoporous Pt shell, J. Am. Chem. Soc. 132 (2010) 13636–13638.
[38] B. Jiang, C. Li, M. Imura, J. Tang, Y. Yamauchi, Multimetallic mesoporous spheres through surfactant-directed synthesis, Adv. Sci. 2 (2015) 1500112.
[39] B.P. Bastakoty, Y. Li, S. Guragain, S.M. Alshehri, M.J.A. Shiddiky, Z. Liu, K. Shim, J.H. Kim, M.S.A. Hossain, V. Malgras, Y. Yamauchi, Formation of mesopores inside platinum nanospheres by using double hydrophilic block copolymers, Mater. Lett. 182 (2016) 190–193.
[40] L.L. Israel, E. Lelloushe, S. Ostrovsky, V. Yarmiayev, M. Bechor, S. Michaeli, J.-P.M. Lellouche, Acute in vivo toxicity mitigation of PEI-coated maghemite nanoparticles using controlled oxidation and surface modifications toward siRNA delivery, ACS Appl. Mater. Interfaces 7 (2015) 15240–15255.
[41] M. Pasenkiewicz-Gierula, Y. Takaoka, H. Miyagawa, K. Kitamura, A. Kusumi, Charge pairing of headgroups in phosphatidylcholine membranes: a molecular dynamics simulation study, Biophys. J. 76 (1999) 1228–1240.
[42] N.-H. Kwon, K.-S. Lee, M.-S. Won, Y.-B. Shim, An all-solid-state reference electrode based on the layer-by-layer polymer coating, Analyst 132 (2007) 906–912.
[43] D.-M. Kim, S.-J. Cho, C.-H. Cho, K.-B. Kim, M.-Y. Kim, Y.-B. Shim, Disposable all-solid-state pH and glucose sensors based on conductive polymer covered hierarchical AuZn oxide, Biosens. Bioelectron. 79 (2016) 165–172.
[44] K. Shim, J. Kim, Y.-U. Heo, B. Jiang, C. Li, M. Shahabuddin, K.C.-W. Wu, M.S.A. Hossain, Y. Yamauchi, J.H. Kim, Synthesis and cytotoxicity of dendritic platinum nanoparticles with HEK-293 cells, Chem. Asian J. 1 (2017) 21–26.
[45] M.J.A. Shiddiky, Y.-B. Shim, Trace analysis of DNA: preconcentration separation, and electrochemical detection in microchip electrophoresis using Au nanoparticles, Anal. Chem. 79 (2007) 3724–3733.
[46] M.A. Rahman, A. Kothalam, E.S. Choe, M.-S. Won, Y.-B. Shim, Stability and sensitivity enhanced electrochemical in vivo superoxide microbiosensor based on covalently co-immobilized lipid and cytochrome c, Anal. Chem. 84 (2012) 6654–6660.
[47] N.G. Gurudatt, M.H. Naveen, C. Ban, Y.-B. Shim, Enhanced electrochemical sensing of leukemia cells using drug/lipid co-immobilized on the conducting polymer layer, Biosens. Bioelectron. 86 (2016) 33–40.
[48] H. Zhu, A. Sigdel, S. Zhang, D. Su, Z. Xi, Q. Li, S. Sun, Core/shell Au/MnO nanoparticles prepared through controlled oxidation of AuMn as an electrocatalyst for sensitive $H_2O2$ detection, Angew. Chem. Int. Ed. 53 (2014) 12716–12720.
[49] M.H. Naveen, N.G. Gurudatt, H.-B. Noh, Y.-B. Shim, Dealloyed AuNi dendrite anchored on a functionalized conducting polymer for improved catalytic oxygen reduction and hydrogen peroxide sensing in living cells, Adv. Funct. Mater. 26 (2016) 1590–1601.
[50] Y. Zhang, L. Wang, D. Lu, X. Shi, C. Wang, X. Duan, sensitive determination of bisphenol a base on arginine functionalized nanocomposite graphene film, Electrochim. Acta 80 (2012) 77–83.
[51] M. Portaccio, D.D. Tuoro, F. Arduini, D. Moscone, M. Cammarota, D.G. Mita, M. Lepore, Laccase biosensor based on screen-printed electrode modified with thionine-carbon black nanocomposite, for bisphenol A detection, Electrochim. Acta 109 (2013) 340–347.
[52] L.A. Goulart, F.C.D. Moraes, L.H. Mascaro, Influence of the different carbon nanotubes on the development of electrochemical sensors for bisphenol A, Mater. Sci. Eng. C 58 (2016) 768–773.
[53] B. Kaur, B. Satpati, R. Srivastava, $ZrO_2$ supported nano-ZSM-5 nanocomposite material for the nanomolar electrochemical detection of metol and bisphenol A, RSC Adv. 6 (2016) 65736–65746.
[54] Y. Zhou, L. Yang, S. Li, Y. Dang, A novel electrochemical sensor for highly sensitive detection of bisphenol A based on the hydrothermal synthesized Na-doped $WO_3$ nanorods, Sens. Actuators B: Chem. 245 (2017) 238–246.
[55] B. Su, H. Shao, N. Li, X. Chen, Z. Cai, X. Chen, A sensitive bisphenol A voltammetric sensor relying on AuPd nanoparticles/graphene composites modified glassy carbon electrode, Talanta 166 (2017) 126–132.
[56] Y.T. Yaman, S. Abaci, Sensitive adsorptive voltammetric method for determination of bisphenol A by gold nanoparticle/polyvinylpyrrolidone-modified pencil graphite electrode, Sensors 16 (2016) 756.
[57] J. Li, D. Kuang, Y. Feng, F. Zhang, M. Liu, Voltammetric determination of bisphenol A in food package by a glassy carbon electrode modified with carboxylated multi-walled carbon nanotubes, Microchim. Acta 172 (2011) 379–386.

## Biographies

**Mr. Kyubin Shim** received his B.S. degree from the department of physics, Pukyong National University, South Korea in 2013. His main research works are mainly the synthesis of porous materials for electrochemical sensing applications.

Please cite this article in press as: K. Shim, et al., Efficient wide range electrochemical bisphenol-A sensor by self-supported dendritic platinum nanoparticles on screen-printed carbon electrode, Sens. Actuators B: Chem. (2017), http://dx.doi.org/10.1016/j.snb.2017.09.096

**Dr. Jeonghun Kim** received his B.S. degree (2007) and Ph.D. degree (2012) from Yonsei University in Seoul, Korea. His major research interest is the design and development of functional organic and inorganic materials for electronic and energy storage applications.

**Prof. Mohammed Shahabuddin** received his bachelor's degree (1983) from University of Bihar Muzaffar and master's degree (1986) and PhD (1993) from Indian Institute of Technology (I.I.T.). His major research interest is in development of functional nanomaterials for various electrochemical applications.

**Prof. Yusuke Yamauchi** received his bachelor's degree (2003), master's degree (2004), and PhD (2007) from the Waseda University in Japan. His major research interest is in the tailored design of inorganic nanostructured materials with various shapes and compositions toward practical applications.

**Dr. Md. Shahriar A. Hossain** received his Ph.D. degree in Materials Science and Engineering from the Institute for Superconducting and Electronic Materials (ISEM), University of Wollongong (2008). His major research interest is in development of mesoporous materials for bio-related applications.

**Prof. Jung Ho Kim** received his Bachelor's (1998), Master's (2000), and PhD (2005) degrees from Sungkyunkwan University, Korea. His major research interest is in the rational design of materials with one-, two-, and three-dimensions towards energy storage and harvesting applications.

Please cite this article in press as: K. Shim, et al., Efficient wide range electrochemical bisphenol-A sensor by self-supported dendritic platinum nanoparticles on screen-printed carbon electrode, Sens. Actuators B: Chem. (2017), http://dx.doi.org/10.1016/j.snb.2017.09.096